A Ground-Based Differential Absorption (DIAL) Lidar For Boundary Layer Profiling of CO_2

Co-Principal Investigators: Arlyn E. Andrews and John F. Burris

Co-Investigators: Michael A. Krainak, Haris Riris, Xiaoli Sun, James B. Abshire, and G. James Collatz

Abstract:

We propose to develop and demonstrate a transportable ground-based Differential Absorption Lidar (DIAL) system, in breadboard form, which is capable of providing continuous measurements of CO_2 profiles through the PBL. This will address a critical limitation of the existing network for monitoring global CO_2 distributions, which is comprised mainly of surface flask sampling sites at remote marine locations.

We propose to assemble and characterize a mobile breadboard DIAL profiling lidar that can be operated from a modified cargo van. We will measure atmospheric CO_2 profiles under a wide range of conditions from our lab at GSFC. We plan to characterize the lidar's performance in 2005 with two field intercomparison missions at the WLEF-TV tall tower CO_2 monitoring site in Park Falls, WI. These deployments will be coordinated with anticipated activities under the North American Carbon Program. Our calculations indicate that the breadboard lidar should achieve measurement precision of 1 ppmv or better for hourly profiles spanning the PBL. Our lidar approach uses compact, rugged, off-the-shelf, commercial lasers and detectors at 1.58 μm that were developed for telecommunications applications. This leverages and is synergistic with ongoing work funded by the NASA Earth Science Technology Office's (ESTO) Advanced Component Technology program to study the feasibility of a satellite-borne CO_2 laser sounder ("Laser Sounder for Remotely Measuring Atmospheric CO_2 Concentrations").

The work proposed for this NRA will demonstrate the performance of the breadboard profiling lidar. Following the micro-pulse lidar concept [Spinhirne, 1993], its design will be practical to replicate in a fully autonomous version for deployment in future CO_2 observing networks. Our breadboard lidar will also provide scientifically useful data in its own right, and a further engineered version could be an important asset for validating future satellite observations of CO_2. Our work will also provide new information about measurement stabilities and component characteristics, which are needed to develop CO_2 laser sounder instruments for satellites.

1. Scientific Motivation:

Accurate observations of atmospheric CO_2 concentrations are needed to identify and quantify processes that control partitioning of carbon among the atmosphere and oceanic and terrestrial reservoirs. The existing network for monitoring global CO_2 distributions is comprised mainly of surface flask sampling sites at remote marine locations. Observations from these sites effectively constrain estimates of the latitudinal distribution of carbon sources and sinks, but the data do not provide sufficient information to infer longitudinally resolved surface fluxes [e.g, Gurney et al., 2002]. Longitudinally resolved measurements are needed, for example, to determine whether the United States is a net source or sink of atmospheric carbon dioxide. A principal objective of the North American Carbon Program is to address the limitations of the current CO_2 observing system by greatly augmenting the existing network [Wofsy and Harriss, 2002].

New and fully representative measurements need to be added in the vicinity of strong terrestrial sources and sinks. Figure 1 shows data from the National Oceanic and Atmospheric Administration Climate Monitoring and Diagnostics Laboratory (NOAA CMDL) "tall tower" monitoring site at the WLEF-TV tower in Park Falls, Wisconsin (45.95 N, 90.27W) for January and July 2000 [Courtesy of Peter Bakwin, see Bakwin et. al, 1998]. July data are characterized by a large diurnal cycle and strong vertical gradients

at night, and CO_2 concentrations in both January and July exhibit large day-to-day variability. Figure 2 shows profiles obtained by an in situ instrument flown over (a) the Amazon Forest and (b) over the Wisconsin NOAA CMDL tower site. In these two cases, diurnal variations are confined to altitudes below 1 km, and the free troposphere above the planetary boundary layer (PBL) is vertically homogeneous and nearly constant throughout the day.

There are two important challenges for obtaining representative measurements over the continents: (1) measurements must be frequent enough to capture strong diurnal variations, and (2) interpretation of surface data is complicated by the covariance of the diurnal cycles of photosynthesis and turbulent atmospheric mixing in the PBL. Existing strategies for overcoming these challenges have important deficiencies. Television towers such as the WLEF-TV tower can be instrumented to provide continuous measurements of CO_2 but are limited to heights less than ~500 meters, while the height of the summertime boundary layer is typically a few kilometers. In situ CO_2 analyzers flown on light aircraft are capable of sampling the entire depth of the boundary layer, but practical considerations dictate that routine sampling will be relatively infrequent (~weekly) and limited to daytime fair-weather conditions.

Lidar systems have the capability of providing continuous vertical profiles of trace gas concentrations through the depth of the PBL, thus addressing both of the key sampling issues for CO_2 over the continents. We seek to develop and characterize such a profiling CO_2 lidar. Our approach leverages prior NASA investments in laser techniques for remotely measuring CO_2.. Our breadboard lidar can serve as a prototype for a fully autonomous lidar, which would be suitable for duplication by a commercial organization (e.g., under the Small Business Innovation Research or Small Business Technology Transfer Programs) and deployment in a CO_2 observing network.

Most continental CO_2 observations have been made in forested regions, away from the influence of urban centers. Our location at the NASA Goddard Space Flight Center (GSFC) just outside of Washington, DC offers a unique vantage point for observing CO_2 mixing ratios. As a part of this effort, we plan to use atmospheric transport models to analyze CO_2 concentrations at GSFC in relation to factors such as traffic patterns and energy demand, in addition to parameters such as photosynthetically active radiation, leaf area index, temperature, and precipitation, which are important for estimating biospheric fluxes. To date, model simulations of CO_2 have relied on an annually averaged fossil fuel emissions estimates based on economic and population data [Andres et al., 1996; Brenkert]. These estimates have important limitations. Global gridded estimates are available only for 1990 and 1995, and fluxes are distributed according to population rather than where the emissions are generated (for example large power plants outside of major population centers are not well represented). Currently available estimates also do not account for seasonal variations in energy demand. As more high frequency measurements of CO_2 over the continents become available, and models are developed that solve for carbon uptake at finer spatial and temporal scales, better information about anthropogenic emissions will be needed.

Data from a Licor 6262 CO_2/H_2O analyzer, which was recently installed in our laboratory, provides an indication of atmospheric CO_2 concentrations in the vicinity of GSFC (Figure 3&4). The instrument samples air drawn in through an inlet on the roof. Data obtained during early October indicate a strong diurnal cycle, presumably due to a combination of photosynthetic uptake of CO_2 and entrainment of free tropospheric air as the PBL grows over the course of the day. Data obtained just over a month later, after the trees had lost their leaves, do not have a strong daily cycle. Background values during this time period are quite high, and large day-to-day variations are present, perhaps indicating increased accumulation of pollution due to less vigorous vertical mixing during this time period coupled with the lack of photosynthesis.

Applicability to NASA Objectives: The proposed work is directly relevant to NASA's Earth Science Enterprise and to the call for improved observations of carbon cycle gases outlined in the current NRA. This effort will both leverage and complement ongoing work under the Advanced Technology Initiative (ATI) project "Laser Sounder for Remotely Measuring Atmospheric CO_2 Concentrations" [Abshire et al., 2001; Andrews et al., 2002; Sun et al., 2002]. The objective of that work is to investigate the feasibility of measuring CO_2 column abundance with a satellite-borne laser sounder, which will monitor absorption by

CO_2 of laser light transmitted from a satellite and reflected by Earth's surface. Future laser-based satellite observations of CO_2 will have several advantages over passive CO_2 sensors that measure reflected sunlight: (1) measurements can be made at night as well as day, so an orbit can be selected to minimize biases from the diurnal cycle of CO_2 (2) the atmospheric sampling geometry is always a simple fixed 2-way vertical path, (3) the instrument's wavelength control and stability are practical at the 0.01 pm (1 MHz) level, and (4) photons that are backscattered from aerosols and thin clouds in the field of view can be unambiguously detected and rejected. The measurement approach for the ground-based profiler is very similar to that for the satellite-borne laser sounder, but the profiler will make range resolved (i.e., vertical profile) measurements using light backscattered from aerosol particles suspended in the atmosphere. Most of the critical system components for the profiler are identical to those being considered for the laser-sounder. By using hardware provided primarily by the ATI effort and choosing a mobile breadboard configuration, we will be able to thoroughly investigate the potential of lidar measurements at 1.58 μm to contribute to future CO_2 observing networks at minimal cost. At the same time, the profiler application will help advance many of the laser sounder objectives. For example, component performance and durability will be measured under both lab and field conditions. This will provide an excellent opportunity for validation of the transmitter's wavelength and measurement stability and the overall measurement performance versus time.

The Orbiting Carbon Observatory (OCO) was recently selected under the NASA Earth Systems Science Pathfinder (ESSP) program. It is planned to be the first satellite instrument dedicated to measuring atmospheric CO_2 abundance, with a nominal launch date of 2006. The stringent measurement requirements and potential for systematic biases [Kuang et al., 2002; Rayner et al., 2002] dictate that a rigorous validation effort will be required. Current validation plans for OCO call for surface concentration measurements combined with aircraft profiles from in situ sensors and upward looking high-resolution spectrometers. Once demonstrated, our profiler will be well-suited for duplication and deployment in a network configuration. The addition of profiling lidar instruments to the OCO validation strategy would fill a critical intermediate gap in connecting routine surface observations to the total column measurements provided by the spectrometers.

2. Approach:

A Light Detection and Ranging (LIDAR) system measures laser light backscattered from molecules and/or atmospheric aerosol particles [e.g., Browell et al., 1998; McDermid et al., 1991; Measures, 1984]. The key components of a lidar are the laser transmitter, receiver (telescope), and detection system. To obtain vertically resolved data, the laser is typically pulsed and photons are separated into time-resolved range bins based on the "time-of-flight" for photons to travel from the transmitter and be scattered back to the receiver. The relative number of detected photons in the range bins provides a vertical profile. The time width of the laser pulse determines the minimum vertical resolution achievable for a given system, while the time between successive pulses determines the maximum altitude that can be sampled for unambiguous range separation (i.e., so that photons scattered from different heights do not reach the detector at the same time).

We propose to use Differential Absorption Lidar (DIAL) to profile CO_2 within the planetary boundary layer. We will use two lasers operating at separate but closely spaced wavelengths in the CO_2 vibrational-rotational absorption band near 1.58 μm (Figure 5). This absorption band falls within the telecommunications "L-band," allowing us to leverage the private sector's investment in developing semiconductor lasers, fiber amplifiers, detectors, and other instrument components optimized for this wavelength region. The wavelength is also within an 'eye safe' region of the optical spectrum making it suitable for a "no-hazard and eye safe" autonomous lidar.

The CO_2 absorption band consists of discrete, narrow lines closely spaced in wavelength. The "on-line" channel of the sensor, tuned to 1570.824 nm, experiences significant absorption by CO_2, while the "off-line" channel (offset by ~0.15 nm) provides a measure of the background transmittance. The strong differential attenuation of the two channels provides high sensitivity to small variations in CO_2. This

spectral region is nearly free from interference from H_2O and other molecules, and the narrow separation between the on and off-line laser wavelengths minimizes differences in transmittance due to factors other than CO_2 absorption. Rayleigh scattering alone is too weak at these wavelengths to provide adequate signal returns for the proposed system. However, Mie scattering from boundary layer aerosols, with backscattering coefficients that range from 10^{-7} to $>10^{-6}$ m^{-1} sr^{-1} at 1.58 μm will provide sufficient returns (Figure 6; see also Chudamani et al. [1996] and Srivastava et al. [2001]).

We have minimized the temperature sensitivity by selecting a line near one of the inflection points where the temperature dependence changes sign (Figure 5c). The residual temperature dependence is small, but non-negligible, a 0.1-0.3 ppmv error in the calculated CO_2 mixing ratio would result for each degree error in temperature (Figure 5d). We will evaluate and characterize the impact of this error source as part of this work. If needed, we will explore approaches to correct for the error by using 2 lines with different temperature sensitivities.

There is also a residual error from the "dilution effect " of water vapor. For carbon cycle studies we want to determine the CO_2 mixing ratio with respect to dry air (i.e., molecules of CO_2 per million molecules of O_2+N_2). When surface pressure is used as a reference, what is actually calculated is the mixing ratio with respect to wet air (O_2+N_2+H_2O). This is a common problem for any method of measuring CO_2 that does not explicitly incorporate a separate measurement of either water vapor or of an indicator of the dry air abundance such as O_2. Typically, the mixing ratio of water vapor must be known to within 10% in order to calculate a sufficiently accurate dry air mixing ratio. In the near term, we will obtain water vapor data from a water vapor Raman lidar located at GSFC [Whiteman et al., 2001]. In the longer term, either an H_2O channel or an O_2 channel could be added to the proposed instrument. We will evaluate the need for an O_2 channel as part of this work.

A block diagram of the proposed profiler is shown in Figure 7. Items for which we are requesting funding are indicated by the green dashed boxes. Figure 8 shows many of the components already available in our lab and our current setup for hard-target testing, and initial measurements of atmospheric CO_2 using the test setup are shown in Figure 9. The majority of the hardware was purchased under the ATI laser-sounder effort with funding for a few profiler-specific components provided by internal funding from GSFC. As listed in Table 1, the total NASA investment in components already in our lab exceeds $160,000.

Measurement requirements: The data shown in Figures 1-3 provide an indicator of the measurement precision required to resolve the variability in atmospheric CO_2. Strong seasonal and diurnal variations are observed at the surface, but the amplitudes of these variations are damped rapidly with altitude. Our proposed profiling lidar will have a selectable range resolution from <125 to 300 meters. The pressure-weighted average CO_2 value for the vertical column sampled at the WLEF tower site (11-396m) provides a reasonable indicator of the range of CO_2 mixing ratios that would be sampled by the lowest altitude bin of our proposed lidar system (Figure 10). The amplitude of the diurnal cycle in July is ~15 ppmv, while day-to-day variations in February span ~8 ppmv. Evidence of the seasonal cycle is also seen in this plot. The mean values for February and July are separated by ~10 ppmv. In order to resolve these variations, precision better than 1 ppmv (0.3%) is desirable. As summarized in the performance section below, our performance calculations indicate that our proposed lidar should be able to achieve this precision.

***Laser Transmitter*:** CO_2 has discrete absorption lines in the 1.58 μm region. Thus, a narrow single mode laser is required to minimize uncertainties in the effective absorption cross section. To limit this error to < 0.1%, the laser's time averaged linewidth must be < 20 MHz. Two Distributed Feed Back (DFB) lasers will be employed (Figure 8a), one for the on-line and one for the off-line wavelength. Commercially available DFB lasers developed for telecommunications applications are compact, efficient and reliable. These lasers provide single mode output and have typical linewidths of less than 1 MHz. The on-line laser can readily be locked to the required CO_2 line using a gas cell and standard diode frequency locking techniques [Riris et al., 1994; Yoshitake et al., 1993].

Range resolved CO_2 measurements require that both the on and off line signals be pulsed. We will employ an Acousto-Optic Modulator (AOM) to achieve pulse repetition rates in excess of 150 KHz. Actual

switching times between wavelengths will be tailored to take into account local observational conditions. To achieve sufficient output energy, the pulsed outputs from the AOMs will be injected into a common Erbium Doped Fiber Amplifier (EDFA, Figure 8b). EDFAs, like DFB lasers, are commercial products, and their use as high-fidelity power amplifiers has been validated by the telecommunications industry. Single mode output powers of 10 watts continuous wave (CW) are readily available using commercially available EDFAs [Baggett et al., 2001,Champert et al., 2001, Monro et al, 2001, Renaud et al., 2001]. Figure 11 shows a scan of the CO_2 absorption line at 1571.11 nm performed under the ATI laser sounder effort; there is no evidence of spectral broadening at the highest output power used, 5.3W.

To generate pulses from the CW output of an EDFA requires that the signal be modulated. To maximize the available output power, the laser should be operated at the highest possible repetition rates. Our design uses one laser amplifier and one detector for both the on-line and off-line wavelengths, requiring that the transmitter alternate between on and off line signals. The optimal rate can be determined by examining the maximum round trip time for a pulse to propagate to and scatter back from the top of the PBL.

The daytime summer PBL seldom extends above 3 km, corresponding to a time between pulses of ~20 μsec. This permits both DFB lasers to operate at repetition rates >25 KHz and thereby maximizes the effective duty cycle. The nighttime PBL normally extends no more than several hundred meters so laser repetition rates of up to ~150 KHz can be realized (for a height of 500 meters). Pulse widths are adjustable, and a study of the potential trades among pulse width, vertical resolution and measurement precision will be carried out under various atmospheric conditions. To exclude scattering of the laser beam by clouds or aerosol layers above the PBL (including high altitude cirrus), the laser beam's direction of propagation can be angled with respect to the telescope's field of view (FOV) to insure that overlap does not extend beyond ~3 km altitude. A small aerosol lidar will be collocated with the CO_2 instrument to identify the top of the boundary layer and help optimize the fiber laser's repetition rate. At GSFC, this data can be provided by the MPLNET sensor [E. J. Welton, PI]. As part of this work, we will determine if the profiler might require the addition of an inexpensive aerosol transmitter and detector for future fielded versions.

Receiver/Detector*:* The receiver will use a commercially available 40 cm diameter Cassegrain telescope (Meade Instruments) with modifications to enhance its IR performance. A smaller telescope from our current hard-target setup is shown in Figure 8c, and the 40 cm diameter telescope is currently on order. The mirrors will be gold coated for maximum reflectivity at 1.58 μm, and the corrector plate will be AR coated to minimize reflection losses within this wavelength region. The telescopes will be fiber coupled to a broadband filter (~1.2 nm bandpass) and etalon (~40 pm bandpass) to minimize the solar background count rate during daytime operations. The signal will then be imaged onto the photocathode of an IR photomultiplier tube (PMT) which has quantum efficiency of ~2% at 1.58 μm (Hamamatsu R-5509, Figure 8d). A PMT of this type has been purchased and tested under the ATI laser-sounder project. The dark count rate is ~200,000 counts/second when cooled to 190 K. With this PMT, the lidar system's calculated overall detection efficiency, including losses associated with the optics as well as the 2% quantum efficiency, is estimated to be ~0.01.

Daytime operation will require a compromise between the telescope's field of view (FOV) and the altitude at which the telescope's FOV completely overlaps the laser beam. Small FOV's are desirable during daytime because they significantly reduce background count rates. However, reducing the FOV increases the altitude at which complete overlap with the transmitted laser beam occurs. For example, a 2 mrad FOV for the 40cm telescope will result in complete overlap with the upward propagating laser beam at ~400 meters. In order to obtain complete coverage of the PBL, a second small 10 cm diameter telescope will be used to provide coverage within this region.

Acquisition and control: Data acquisition and control will utilize LabView software in a PC/Mac environment and be modeled after the successful approach currently used on the AROTEL instrument [Heaps and Burris, 1996]. Analog detection using 12-bit A/D boards will be used for the low altitude. Photon counting using high speed (300 MHz) amplifiers, discriminators and multi-channel scalers will be employed above ~500 meters. Shot by shot signal processing will be used to minimize the effects of rapid

atmospheric variations upon the data. All of the necessary detection electronics are commercially available.

Calibration Strategy: In practice, the limiting accuracy that can be obtained by averaging sequential measurements is determined by systematic drifts [Werle, et al., 1993]. We intend to minimize the errors from such drifts by frequent calibration. As shown in Figure 7, our calibration approach has three elements: (1) Fluctuations in transmitter power and detector response will be measured by periodically placing a retroreflector-attenuator assembly into the beam path to reflect a portion of the transmitted light back into the receiver telescope. This will provide a direct "null path" measurement of the background signal levels in the absence of CO_2 absorption. Null profiling can also be accomplished by tuning both lasers to a common wavelength, this will help identify systematic errors originating with the lasers, optical elements or detector chain [Proffitt, 1997].

(2) Two reference cells, each containing pure CO_2 at a different pressure will be utilized to monitor the total span and offset of the absorption measurements. This calibration mode will be a sensitive indicator of signal degradation associated with wavelength drifts or time-averaged line broadening. Differences in the line shape between the pure CO_2 cells and the pressure -broadened atmospheric line will be handled by the algorithm.

(3) Ambient air will be drawn into a third multipass cell with 200-300m path-length. The CO_2 absorption in this volume measured by the lidar (via the retro-reflector assembly) will be compared directly to values measured by a calibrated Licor CO_2 analyzer with a collocated inlet.

Portability: Our breadboard lidar will be developed to allow operation from a remote field location. Our use of fiber lasers provides a small, compact, rugged and energy efficient transmitter. The entire package (consisting of the transmitter, receiver, detection hardware and data acquisition system) will be built onto a small optical table that can be rolled onto the existing Code 924 branch van for deployment. Modifications to the van will be made to allow lidar operation from within the cargo area. These enhancements include a roof hatch and power and data connections, as well as an air conditioning and/or heating unit. The lidar will be initially operated within our building, and it can be rolled to and from the van as a fully operational package.

3. Performance:

Results from a set of calculations to estimate the expected performance of the proposed lidar are shown in Figure 12 for a range of conditions and the corresponding parameters are given in Table 2. These cases were chosen to provide an idea of available design trades. For example, vertical and temporal resolution can be sacrificed to obtain increased precision. The CO_2 mixing ratio and PBL aerosols were assumed to be well mixed for these simulations and the atmospheric density profile was taken from U.S. Standard Atmospheres, 1976. The pressure dependence of the cross section as a function of altitude was included.

Cases A and B are identical except for the values of β_{aer}, which reflect the range of expected values for the PBL over GSFC based on measurements obtained from MPLNET (Figure 6a&b). Above 1 km, performance is marginal for Case B ($\beta_{aer} = 1.6 \times 10^{-7}$), but a precision better than 2 ppmv at 3 km should be possible for the prototype system under conditions of high aerosol loading. Precision of better than 1 ppm is possible for altitudes < 1 km even for low aerosol conditions. The probability distributions shown in Figure 6b indicate that values of $\beta_{aer} > 10^{-6}$ are relatively common in summer, when PBL heights are most likely reach altitudes >1 km.

Cases C-F show the impact of increasing the pulse repetition rate. Increased precision is achieved because the laser power is being used more effectively. However, the maximum altitude that can be sampled is reduced, since photons returning from higher altitudes can interfere with returns originating from subsequent pulses at lower altitudes. This can be avoided by aligning the telescope relative to the receiver in such a way as to exclude photons scattering from higher altitudes. Maximum altitudes were chosen that roughly correspond to average PBL heights during the day (1000 m) and at night (500 m). The PBL can clearly be seen in Figures 6c and 6d, which show the altitude distribution of backscatter from MPLNET at

523 nm for "typical" clear days in January and July over GSFC. These figures include both aerosol and molecular backscatter, but the vertical structure and large values at low altitudes primarily reflect the aerosol contribution. Due to the large dark count rate associated with the PMT (200,000 cts/sec), simulations using the same PBL height and resolution (not shown here) indicated only small differences between day and nighttime performance

Cases G and H shows the performance we expect for a future lidar (Figure 12a). Here we assumed high power fiber amplifiers and improved photon counting detection efficiencies. The calculated precision for Case G includes both Rayleigh scattering and relatively high aerosol loading. Precision is better than 0.5 ppmv for a 10 minute averaging time at 3km. Case H assumes only Rayleigh scattering, and precision better than 1.5 ppmv is possible at 3 km. This implies that measurements could be obtained even for very low aerosol loading and that coverage could be extended to provide a free tropospheric value in addition to profiles throughout the boundary layer. Note that averaging times could be increased or vertical resolution sacrificed to obtain higher precision if desired.

The specifications used in Cases G and H are reasonable if using newly developed components. The laser powers are attainable with currently available technology. Research efforts are currently underway to extend EFDA output powers to several tens of watts while maintaining stable, single mode, operation. The laser sounder proposes to use these or several EDFAs operating in parallel with pre-amplification. These techniques could be applied for a future profiler, but would require obtaining additional hardware. Recent studies show that quantum efficiencies of 20% with low dark counts can be achieved in the 1.5 μm region with cooled APDs [Maruyama et al., 2002; Prochazka and Peltier, 2001], and a commercial version optimized for a slightly shorter wavelength region is already available (Hioki E. E. Corporation). These devices can be cooled using a closed cycle cooler and are more compact and rugged than PMTs. Although the components are becoming available, designing and building such an optimal lidar for remote deployment is a larger research effort requiring more investment than we are asking for here.

Our goal for this work is to use our existing hardware to demonstrate the technique and characterize the measurements. We plan to assess the breadboard profiler's measurements several different ways. Horizontal column measurements over distances of several hundred meters will be carried out using a hard target reflector and compared against data obtained from a collocated in situ CO_2 instrument (Licor 6262, Figure 4). This will allow the lidar's sensitivity to be characterized against diurnal changes in CO_2. We will cross check the measurement sensitivity by comparing the column amounts derived using strong returns from the bottom of clouds to those derived from integrated range resolved profiles. During the third year of the effort the instrument will be deployed for two, three-week, field validation missions at the WLEF-TV NOAA CMDL tall tower monitoring site. This will allow detailed comparisons against the in situ sensors on the tower. The breadboard profiler can be aligned so that its sampling is restricted to altitudes below 500 m. The higher count rates from low altitude backscatter will permit the use of much higher pulse repetition rates and smaller laser pulse widths (smaller range bins) thereby allowing the best comparison with the tower measurements. Accurate temperature and H_2O data are available from the tower, greatly simplifying the comparisons and enabling detailed quantitative assessment of uncertainty in measured CO_2. A letter from Dr. Peter Bakwin expressing his support for the proposed work and his commitment to facilitating the intercomparision study at the WLEF-TV tower is attached.

4. Relationship to Current and Planned ESTO Laser Sounder Activities:

Current support from ESTO for the laser sounder activities is scheduled to conclude during July 2003. At that time we expect to have made calibrated hard-target measurements for the horizontal path from our lab and also using a non-cooperative target. Our proposed profiler work will focus on obtaining range-resolved measurements from aerosol backscatter and on developing an augmented calibration system. We will also address measurement and operation stabilities so that the whole system is transportable and can be operated from the branch van.

The profiler objectives are synergistic with our laser sounder effort, since both require a very stable absorption reference system and both will require range-resolved detection (for the sounder, range-resolved

measurements are needed to detect and reject photons that are scattered from cloud or aerosol layers). We will propose for continued laser sounder work with ESTO. That work will likely focus on component development and measurement demonstrations with advanced components. Those include fiber amplifiers with higher peak powers and higher sensitivity, smaller detectors. We will also request support for the laser sounder's O_2 channel. We will incorporate improved components developed under continuing sounder work into the profiler as their development schedules permit.

5. Facilities:

Through support from the ESTO ATI and Goddard IR&D programs, we have already acquired the majority of the hardware and test equipment needed for breadboard lidar. Goddard has also provided internal funding for the profiler-specific receiver telescope. A Licor 6262 CO_2/H_2O analyzer has been purchased for validation experiments under the Laser Sounder effort along with related automated calibration equipment, pressure and flow controllers and data acquisition hardware. A Nicolet Nexus 870 FTIR, purchased though Goddard general purpose equipment funding, is available for detailed examination of gas spectra and cross comparisons. Our lidar lab in Goddard's Building 33 has hatches that enable atmospheric measurements along both zenith and horizontal paths. We are also using a state of the art detector characterization laboratory, which was developed for the detectors in the GLAS instrument on the ICESat mission.

We also have access to data from a group of atmospheric sensors located near our building at Goddard. Lidar measurements include water vapor profiles from the Water Vapor Raman Lidar [David Whiteman, PI] and aerosol profiles from the MicroPulse Lidar Network (MPLNET) [E. J. Welton, PI; Spinhirne, 1993]. These provide high vertical resolution backscatter profiles, which allow the determination of aerosol backscatter coefficients and PBL height. Radiometric measurements include those from the Aerosol Robotic Network (AERONET) for observations of the aerosol optical depth and continuous observations of photosynthetically active radiation (PAR) from a radiometer operated by G. Labow.

6. Milestones and Work Plan:

The task plan and milestones for each 3-month work period, and the reporting times are summarized below.

Month after award	Primary Activities	Reporting.
1-3	Measure atmospheric backscatter with 1W peak power & PMT-based receiver	
3-6	Incorporate null path calibration approach; assess CO_2 absorption stability	
6-9	Increase laser to 5 W peak; Incorporate 40 cm telescope into receiver	
9-12	Measure on & off line vertical atmospheric profiles with breadboard.	Year 1 report
12-15	Add one reference cell to calibration system - assess absorption stability	
15-18	Demonstrate full power measurements through PBL from B33	
18-21	Increase laser to 10 W peak; Add 2nd calibration cell; assess stability	
21-24	Move to transportable table; demonstrate performance from B33	Year 2 report
24-27	Remote deployment #1 to the WLEF tower in Wisconsin.	
27-30	Analyze field data; address instrument-related issues	
30-33	Incorporate 3rd calibration cell; retest from building 33.	
33-36	Field experiment #2 at WLEF tower; post experiment data analysis	Final report

7. Investigator Qualifications and Management Plan:

Dr. Andrews has extensive experience making high-precision CO_2 measurements on airplanes and high altitude balloons and analyzing CO_2 data to study atmospheric transport processes. She serves a Co-I on the laser sounder work and has recently become involved with CO_2 simulations in atmospheric transport models at GSFC. She will lead the analysis and assessments of the profiler's CO_2 measurements and help guide the development of the profiler's calibration system.

Dr. Burris has extensive experience with LIDAR measurements of trace gases and atmospheric temperature from both ground and aircraft based platforms. He will serve as the Instrument Scientist for the profiler and coordinate its development. He will share overall coordination and management of the effort with Dr. Andrews.

Dr. Abshire serves as Instrument Scientist and co-led the development of both the MOLA lidar on the Mars Global Surveyor Mission and the GLAS lidar on NASA's ICESat mission. He has experience in developing new laser technologies and measurement techniques for space and other severe environments. He serves as PI on the ESTO ATI laser sounder effort and will be responsible for coordinating ongoing laser-sounder work with the profiler work and will participate in the profiler data analysis.

Dr. Mike Krainak led the development of the GLAS receiver optical filters and detectors and has extensive experience leading and developing new laser and electro-optic technology for lidar. He serves as Co-I on the laser sounder work and will lead the laser and electro-optic developmental efforts for the profiler.

Dr. Haris Riris has extensive experience with tunable diode spectroscopy and laser applications. He was team leader for the new inverse lidar and altimeter used to characterize and calibrate the GLAS instrument. He serves as Co-I on the laser sounder work and will be responsible for tunable diode spectroscopy and absorption calibration subsystem.

Dr. Xiaoli Sun serves as part of the MOLA and GLAS Instrument Science teams and led the pre-flight assessment of their altimetry and lidar performance. He has extensive experience developing and characterizing optical receivers that perform close to the theoretical limits. He serves as Co-I on the Laser Sounder work, and will lead the development of the profiler detector and processing electronics.

Dr. G. James Collatz is an expert on the terrestrial carbon cycle and a Co-I on the laser sounder work. He will participate in profiler data analysis and will provide inputs for numerical simulations of CO_2 fluxes from vegetation and soils.

CVs and pending support information for each investigator are attached at the end of this document.

8. Budget Justification

Complete budget worksheets and summaries are attached. The following is a detailed breakdown for "Program Direct Costs", which is Item 1 on the Budget Worksheets.

	FY03	**FY04**	**FY05**
Long path absorption cell (< 360 meters)	$16 K		
InGaAs photocathode PMT		$25 K	
Cooled Geiger APD and cooler	$15 K		
H. Riris support (0.2MY)	$50 K	$51.2 K	$52.5 K
N. Abuhassam support (0.2MY)	$30 K	$31.2 K	$32.4 K
Mechanical design and fabrication	$10 K	$10 K	$10 K
Optics	$10 K	$10 K	$10 K
Optical design and analysis	$10 K	$10 K	$10 K
Electronics/computer peripheral equipment	$5 K		
Custom mechanical parts		$5 K	
Modifications to branch truck			$6 K
Primary CO_2 standard gases	$ 9.6K		
Working standards for Licor	$1 K	$1 K	$1 K
Licor plumbing supplies	$5 K	$5 K	$5 K
Data analysis computer(2)+ software			
Dew point generator for Licor H_2O channel			$5 K
Reference cells		$17.6 K	
Contractor travel	$2 K	$2 K	$2 K

Total	$163.6	$180.0	$133.9

References:

Abshire J. B., G.J. Collatz, X. Sun, H. Riris, A.E. Andrews, M. Krainak, Laser Sounder Technique for Remotely Measuring Atmospheric CO2 Concentrations, Fall Meeting of the American Geophysical Union, San Francisco, CA, 10-14 December 2001.

Andres, R. J.,Marland, G., Fung, I. &Matthews, E. Distribution of carbon dioxide emissions from fossil fuel consumption and cement manufacture, 1950-1990. Glob. Biogeochem. Cycles **10**, 419-429 (1996).

Andrews, A. E., Burris, J F, Abshire, J B, Krainak, M A, Riris, H , Sun, X G J, "A Ground-Based Profiling Differential Absorption LIDAR System for Measuring Carbon Dioxide in the Planetary" Boundary Layer", Eos Trans. AGU, 83(47), Fall Meet. Suppl., Abstract A12A-0129, 2002.

Baggett J. C., T. M. Monro, K. Furusawa, D. J. Richardson, Comparative study of large-mode holey and conventional fibers, *Optics Lett.,* **26**(14), 1045-1047 (2001).

Bakwin, P. S., et al., Measurements of carbon dioxide on very tall towers: results of the NOAA/CMDL program, Tellus **50B**, 401–415 (1998).

Brenkert, A. L. Carbon dioxide emission estimates from fossil-fuel burning, hydraulic cement production, and gas flaring for 1995 on a one degree grid cell basis. http://cdiac.esd.ornl.gov/ndps/ndp058a.html.

Browell, E.V. et al, Differential absorption lidar (DIAL) measurements from air and space, Appl. Phys. **B67**, 399 (1998).

Champert P.A., S. V. Popov , and J. R. Taylor, Power scalability to 6 W of 770 nm source based on seeded fibre amplifier and PPKTP, *Electronics Lett*., **37**(18): 1127-1129 (2001).
Chudamani S., J. D. Spinhirne and A. D. Clarke, Lidar aerosol backscatter cross sections in the 2 - μm near-infrared wavelength region, Appl. Opt., **35**, 4812 (1996).

Gurney, K., et al.,Towards robust regional estimates of CO_2 sources and sinks using atmospheric transport models, Nature, **415**, 626-630 (2002).

Heaps, Wm. And J. Burris, Airborne Raman Lidar, Appl. Opt., **35**, 7128 (1996).

Kuang, Z., J. Margolis, G. Toon, D. Crisp, and Y. Yung, Spaceborne measurements of atmospheric CO_2 by high-resolution spectrometry of reflected sunlight: An introductory study, Geophys. Res. Lett., **29**, 10.1029/2001GL014298 (2002).

Maruyama, T., F. Narusawa, M. Kudo, M. Tanaka, Y. Saito and A. Nomura, A Development of a near-infrared photon-counting system using an InGaAs avalanche photodiode@, Opt. Eng., **41**, 395 (2002).

McDermid, I. S. et al., Differential absorption lidar systems for tropospheric and stratospheric ozone measurements, Opt. Eng., **30**, 22 (1991).

Measures R., Laser Remote Sensing, John Wiley & Sons, New York, 1984.

Monro T. M., V. Pruneri, N. G. R. Broderick, D. Faccio, P. G. Kazansky, D. J. Richardson, Broad-band second-harmonic generation in holey optical fibers, *IEEE Photonics Tech. Lett.*, **13**(9), 981-983 (2001).

Prochazka, I., Peltier-cooled and actively quenched operation of InGaAs/InP avalanche photodiodes as photon counters at a 1.55 ：m wavelength, Appl. Opt., **40**, 6012 (2001)

Rayner, P. J., R. M. Law, D. M. O'Brien, T. M. Butler, and A. C. Dilley, Global observations of the carbon budget 3. Initial assessment of the impact of satellite orbit, scan geometry, and cloud on measuring CO_2 from space, J. Geophys. Res., **107**, 10.1029/2001JD00018 (2002).

Renaud C. C., H. L. Offerhaus, J. A. Alvarez-Chavez, J. Nilsson, W. A. Clarkson, P. W. Turner, D. J. Richardson, A. B. Grudinin, Characteristics of Q-switched cladding-pumped ytterbium-doped fiber lasers with different high-energy fiber designs, ***IEEE** J. Quantum Electronics,* **37**(2), 199-206 (2001).

Riris, H., C. B. Carlisle, L. Carr, D. E. Cooper, Design of an Open Path Diode Laser Sensor: Application to Water and Oxygen and CO_2 Vapor Detection, Appl. Opt. **33**, 7059 (1994).

Spinhirne, J. D. , Micro Pulse Lidar, IEEE Trans. Geosci. Remote Sen., **31**, 48 (1993).

Srivastava V., J. Rothermel, A.D. Clarke, J. D. Spinhirne, R. T. Menzies, D. R. Cutten, M. A. Jarzembski, D. A. Bowdle and E. W. McCaul, A Wavelength dependence of backscatter by use of aerosol microphysics and lidar data sets: application to 2.1 - μm wavelength for space-based and airborne lidars@, Appl. Opt., **40**, 4759 (2001).

Sun, X. and J. B. Abshire, Performance of a Breadboard Lidar Receiver at 1570nm for Remotely Sensing Atmospheric CO2 Concentration, Conference on Lasers and Electro-Optics (CLEO), Long Beach, California, May 2002.

Whiteman, D.N., K.D. Evans, B. Demoz, D.O'C. Starr, D. Tobin, W. Feltz, G.J. Jedlovec, S.I. Gutman, G.K.Schwemmer, M. Cadirola, S.H. Melfi, F.J. Schmidlin, Raman lidar measurements of water vapor and cirrus clouds during the passage of hurricane Bonnie, *J. Geophys. Res*., **106**(D6), 5211-5225 (2001).

Werle, P., R. Mucke and F. Slemr, The Limits of Signal Averaging in Atmospheric Trace-Gas Monitoring by Tunable Diode-Laser Absorption Spectroscopy (TDLAS), Appl. Phys. B., **B57**, 131 (1993).

Wofsy, S. C. and R. C. Harriss, *The North American Carbon Program (NACP)*, Report of the NACP Committee of the U. S. Interagency Carbon Cycle Science Program. Washington, DC: US Global Change Research Program.

Yoshitake, Satoshi, Akiyama, Koji, Iritani, Miyako, Murayama, Hidekazu, Yokogawa Electric Corp. Publication: Proc. SPIE Vol. 1837, p. 124-133, Frequency Stabilized Lasers and Their Applications, Ken Y. Chung; Ed. Publication Date: 4/1993.

Table 1: Existing investment in laser and electro-optic components from the ESTO Advanced Technology Initiatives Project "Laser Sounder for Remotely Measuring Atmospheric CO_2 Concentrations"

Component	Mfg.	Part No	Price/ea	Quantity	Investment
Wavelength meter	Burleigh	WA-1650	$20,000	1	$20,000
Multipass cell	New Focus		$10,000	1	$10,000
Vacuum pump for cell	Pfiefer		$8,000	1	$8,000
Lock-in Amplifier	SRS	SRS830	$3,650	1	$3,650
Photodiodes	New Focus	2011	$1,090	2	$2,180
Chopper	SRS	SR540	$1,090	1	$1,090
Laser controller	ILX	3722	$5,000	2	$10,000
Seed Lasers	NEC		$2,500	4	$10,000
Fiber couplers	OFR	PAFE-X-1550	$503	4	$2,012
Fiber-pigtailed AO Modulator	Brimrose	N26027-2-1.55	$4,000	2	$8,000
Delay Generator	SRS	DG535	$4,350	1	$4,350
EDFA	IPG Photonics	EAD-5-C	$25,000	1	$25,000
Filter	SRS	SR650	$3,300	1	$3,300
Computer	Dell		$2,500	1	$2,500
Multichannel scalar	SRS	SR430	$7,950	1	$7,950
PMT	Hamamatsu	5509-72	$15,000	1	$15,000
PMT cryostat	IGC Systems	Cryotiger	$8,000	1	$8,000
Receiver Optics			$2,000	1	$2,000
40 cm Cassegrain Telescope	Meade		$18,000	1	$18,000
				TOTAL	$161,037

Table 2: Performance Simulation Parameters.

	Prototype System						**Optimal System**	
	Baseline Cases		Reduced Altitude Cases.					
			Day		Night			
Case	**A**	**B**	**C**	**D**	**E**	**F**	**G**	**H**
β_{aer}, $m^{-1}sr^{-1}$	$1.6x10^{-7}$	$1.6x10^{-6}$	$1.6x10^{-7}$	$1.6x10^{-6}$	$1.6x10^{-7}$	$1.6x10^{-6}$	$1.6x10^{-6}$	0
Energy per Pulse, μJ	16.6	16.6	8.3	8.3	8.3	8.3	200	200
Pulse Width, μs	1.66	1.66	0.83	0.83	0.83	0.83	1.66	1.66
Vertical Resolution, m	250	250	125	125	125	125	250	250
Pulse Rep. Rate, kHz	25	25	62.5	62.5	125	125	25	25
Maximum Altitude, km	3	3	1	1	0.5	0.5	3	3
Detector Quantum Efficiency, %	2	2	2	2	2	2	20	20
Overall Detection Efficiency, %	1	1	1	1	1	1	10	10
Detector Dark Counts, s^{-1}	$2x10^5$	$2x10^5$	$2x10^5$	$2x10^5$	$2x10^5$	$2x10^5$	$2x10^5$	$2x10^5$
Solar Background Counts, s^{-1}	$5x10^5$	$5x10^5$	$5x10^5$	$5x10^5$	0	0	$5x10^5$	$5x10^5$
Averaging Time, min	60	60	60	60	60	60	10	10

Current and Pending Research Support

Other agencies to which this proposal, or parts thereof, has been submitted: ***None***

James Abshire

Principal Investigator	
Proposal Title:	Laser Sounder Technology for Atmospheric CO_2 Measurements from Space
Source:	NASA
Amount:	$150K/year
Period:	5/00 – 5/03
Location:	Goddard
Man years:	0.3

Principal Investigator	
Proposal Title:	Mars Lander Lidar
Source:	NASA
Amount:	$150 K/ year
Period:	2003
Location:	Goddard
Man years:	0.2

ICESat Flight Project Support:	GLAS Instrument Science
Source:	NASA
Amount:	$480 K
Period:	2003
Location:	Goddard
Man years:	0.4

Arlyn Andrews

Co-Investigator	
Proposal Title:	Fabry-Perot Interferometer for Column CO2
Source:	NASA
Amount:	$1400K
Period:	2002-2004
Man years:	0.3

Co-Investigator	
Proposal Title:	Boundary Layer Carbon Dioxide Profiling using Raman Lidar
Source:	NASA
Amount:	$222K (pending)
Period:	2003-2005
Man years:	0.05

John Burris

Principal Investigator	
Proposal Title:	Airborne Raman Ozone Temperature and Aerosol Lidar (AROTEL)
Source:	NSA
Amount:	$255K
Period:	2003
Location:	Goddard
Man years:	0.1

Co-Investigator	
Proposal Title:	Fabry-Perot Interferometer for Column CO2
Source:	NASA
Amount:	$1400K
Period:	2002-2004
Man years:	0.1

G. James Collatz

Co-Investigator
Proposal Title: Land surface hydrological processes: Their representation in global climate models and their impact on precipitation predictability.
Source: NASA
Amount: $120K
Period: 3/2000 –10/2003
Man years: 0.1

Co-Investigator
Proposal Title: The use of satellite fire products and models to investigate the effects of fire on the global Carbon cycle
Source: NASA
Amount: $300K
Period: 3/2000 – 10/2003
Man years: 0.3

Michael Krainak

Co-Investigator
Proposal Title: Laser Sounder Technology for Atmospheric CO_2 Measurements from Space
Source: NASA
Amount: $150K/year
Period: 5/00 – 5/03
Location: Goddard
Man years: 0.2

Co-Investigator
Proposal Title: Mars Lander Lidar
Source: NASA
Amount: $150 K/year
Period: 2001-2003
Location: Goddard
Man years: 0.1

ICESat Flight Project Support: GLAS Detectors
Source: NASA
Amount: $50 K
Period: 2003
Location: Goddard
Man years: 0.2

Haris Riris

Co-Investigator
Proposal Title : Laser Sounder Technology for Atmospheric CO_2 Measurements from Space
Source: NASA
Amount: $150K/year
Period: 5/00 – 5/03
Location: Goddard
Man years: 0.3

ICESat Flight Project Support: GLAS Instrument Science
Source: NASA
Amount: $480 K
Period: 2003
Location: Goddard
Man years: 0.4

Xiaoli Sun

Co-Investigator
Proposal Title : Laser Sounder Technology for Atmospheric CO_2 Measurements from Space
Source: NASA
Amount: $150K/year
Period: 5/00 – 5/03
Location: Goddard
Man years: 0.2

Co-Investigator
Proposal Title: GLAS Instrument Science
Source: NASA
Amount: $480 K
Period: 2003
Location: Goddard
Man years: 0.3

Flight Project Support: Mercury Laser Altimiter
Source: NASA
Amount: $100 K
Period: 2002-2003
Location: Goddard
Man years: 0.2

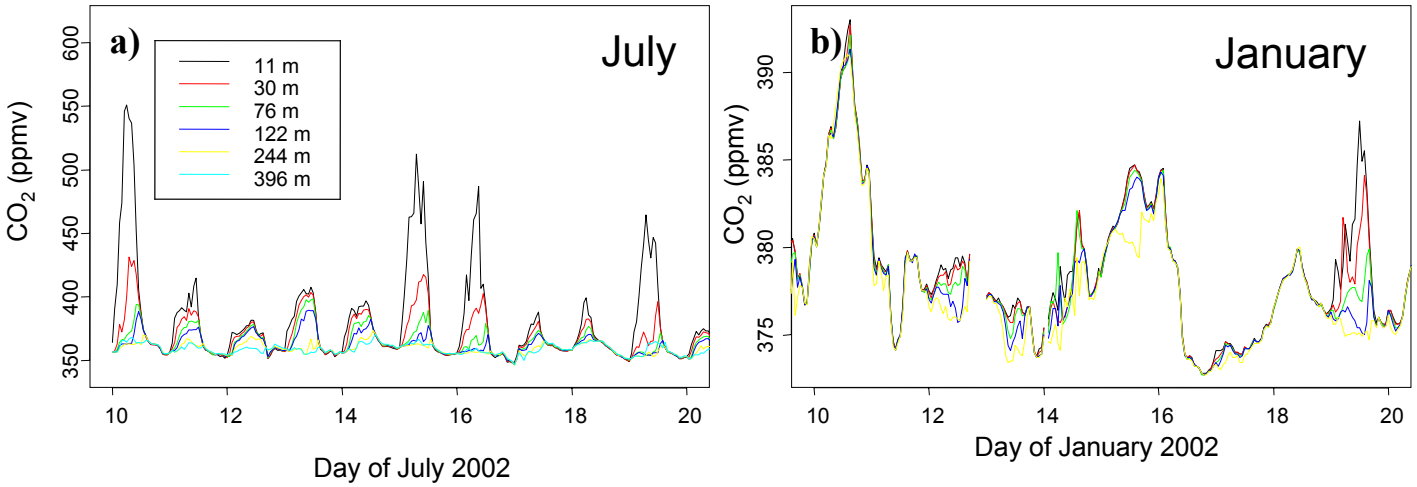

Figure 1. Observed CO_2 mixing ratios at the NOAA CMDL WLEF-TV tall tower monitoring site near Park Falls, WI for two 10 day periods in **(a)** July and **(b)** January 2002. Note the differing scales for the y-axes.

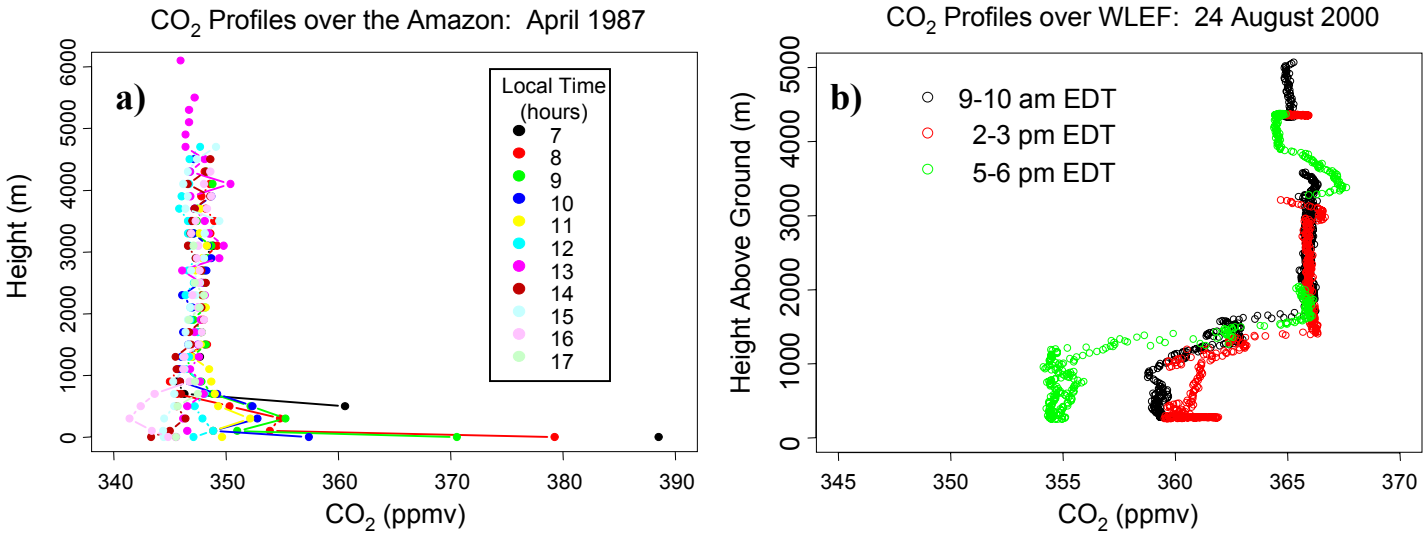

Figure 2. CO_2 profiles obtained using aircraft-borne in situ CO_2 analyzers over **(a)** the Amazon and **(b)** over the WLEF tall tower in Wisconsin. Diurnal variations in the planetary boundary layer are apparent in both plots.

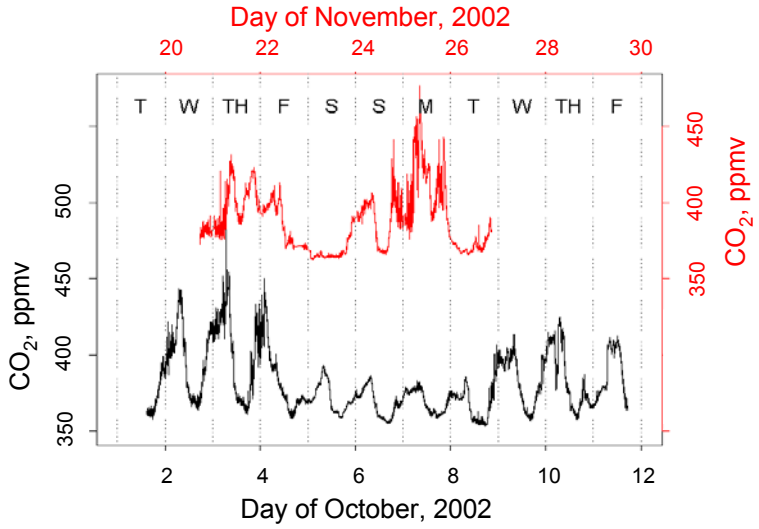

Figure 3. CO_2 measurements obtained using a Licor 6262 CO_2/H_2O analyzer from the roof of our lab at GSFC in Greenbelt, MD during October (black, left axis) and November (red, right axis) 2002. Strong diurnal variations due to photosynthesis are evident in the October data. Large variations are also present in November and may reflect accumulation of pollution from nearby highways.

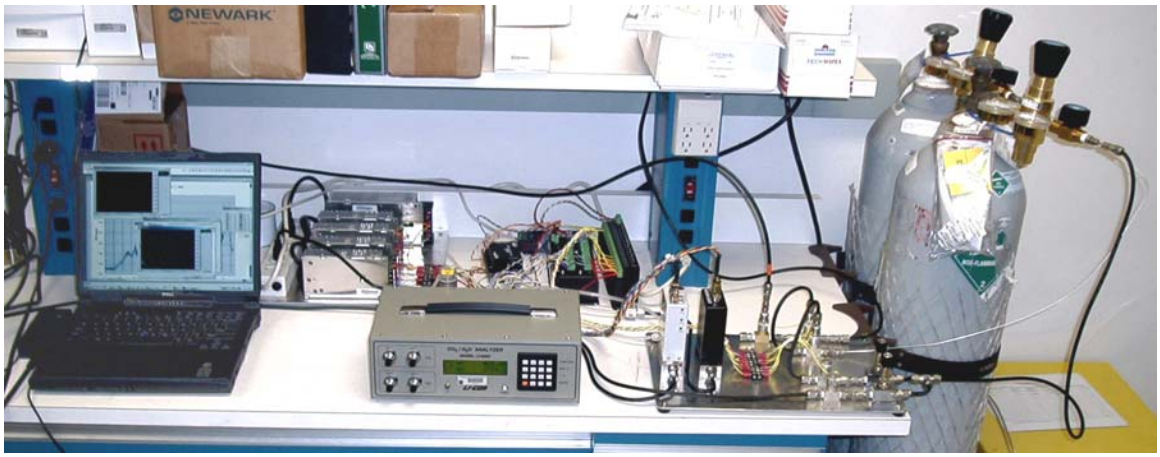

Figure 4. Licor 6262 CO_2/H_2O Analyzer set up with pressure and flow control and automated calibration. A vacuum pump (not shown) is used to draw air through an inlet on the roof of the building shown in Figure 10f.

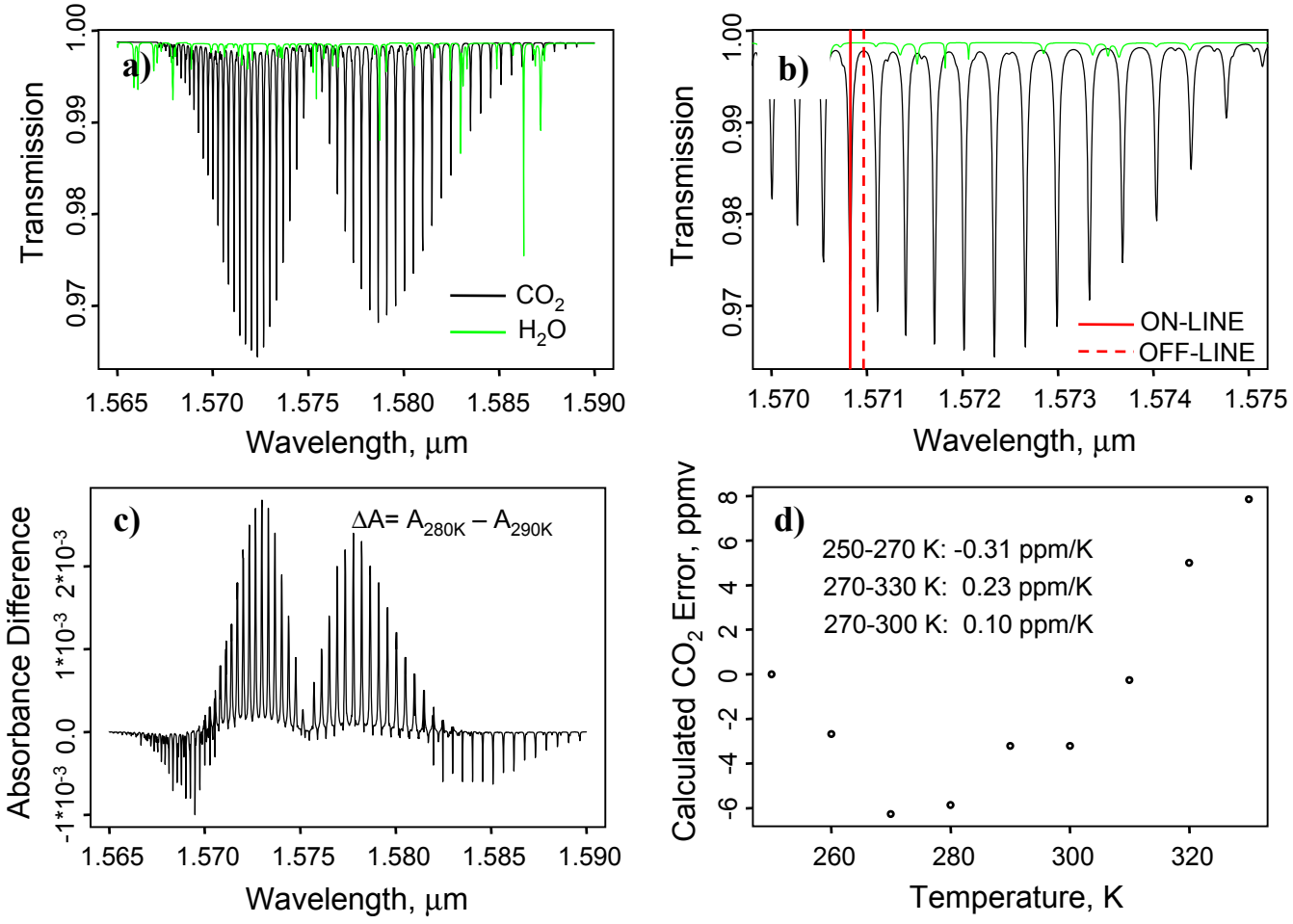

Figure 5. **(a)** Transmission spectra near 1.58μm for CO_2 and H_2O. **(b)** The red vertical lines indicate the on-line (1.5708224 μm) and off-line laser wavelengths for the proposed lidar instrument chosen to avoid interference from H_2O and to minimize temperature sensitivity. **(c)** Calculated difference in absorbance for 280 K and 290 K for a 100 m horizontal path with 330 ppmv CO_2. The selected line lies near one of the inflection points where the temperature dependence changes sign. **(d)** Potential error in CO_2 mixing ratio due to uncertainty in atmospheric temperature for a 200 m range bin with CO_2 = 415 ppm for the line at 1.570822 μm. Error is calculated relative to a simulation where T=250 K.

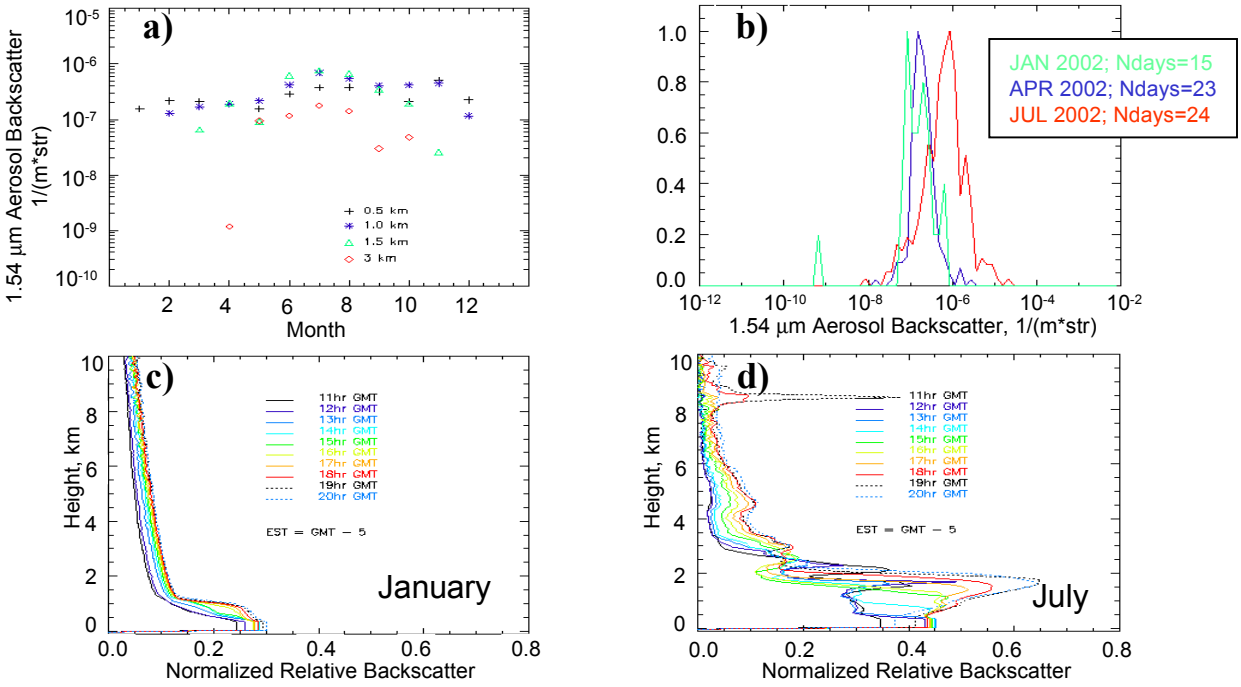

Figure 6. (a & b) Aerosol backscatter coefficients, β_{aer}, for 1.54 µm inferred using relationships given by Srivastava et al. [2001] with data at 523 nm from the Micro-Pulse Lidar Network (MPLNET) instrument at GSFC[Courtesy of E. J. Welton]. Note that values are currently available only for clear-sky daytime conditions when coincident measurements of aerosol optical depth are available from co-located AERONET radiometers. **(a)** Monthly median values for four different heights. **(b)** Probability distribution for β_{aer} at 1 km for January, April and July 2002. The y-axis scale is arbitrary. **(c & d)** Normalized relative backscatter (NRB) from MPLNET for a representative clear day in **(c)** January and **(d)** July. NRB includes both Rayleigh and aerosol backscatter at 523 nm; it is shown here to provide an indication of the height and diurnal growth of the PBL.

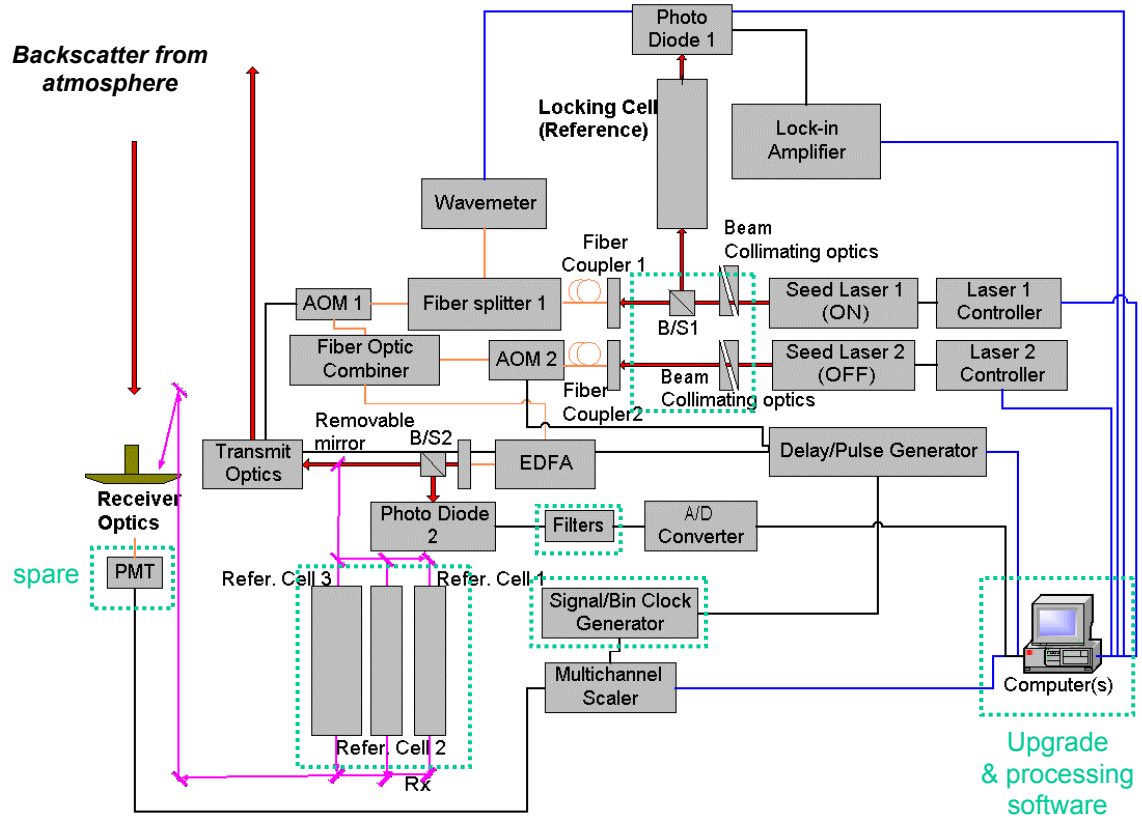

Figure 7. Schematic of the transmitter and receiver for the profiling lidar. Components to be purchased or developed for this proposal are indicated by dashed green boxes. The remaining components have been acquired using funds from the ESTO ATI Program or Bid & Proposal funding from GSFC. The major existing components are listed in Table 1. Note that the various coupling optics and mounts, and optics required for the low altitude receiver telescope are not shown (see text).

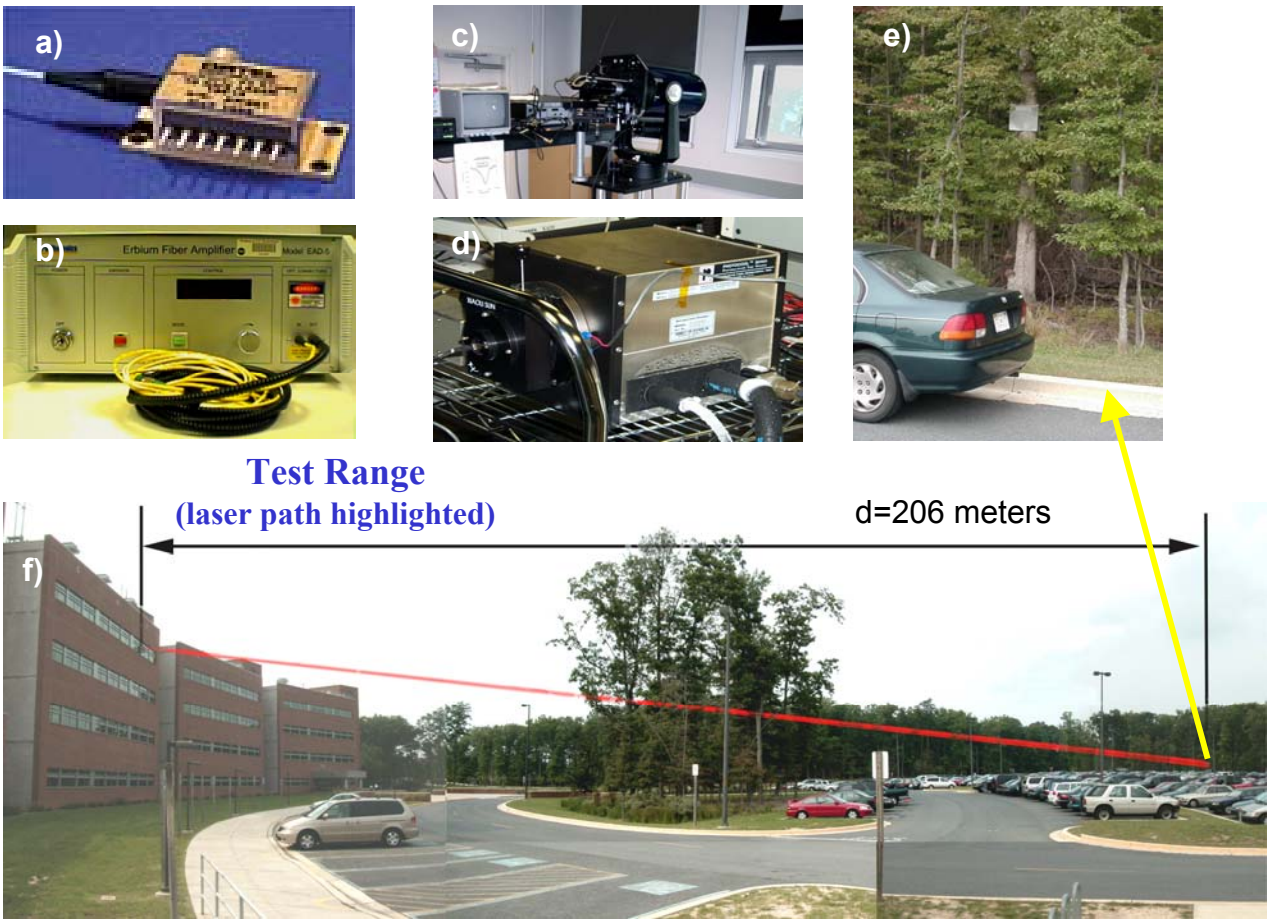

Figure 8. Key system components acquired under the ESTO ATI Program and current setup for hard target measurements at GSFC: **(a)** Distributed Feedback (DFB) tunable semiconductor seed laser, **(b)** Erbium-Doped Fiber Amplifier (EDFA), **(c)** 8" telescope **(d)** PMT, **(e)** reflective target, **(f)** hard-target test range showing laser path from laboratory window to target.

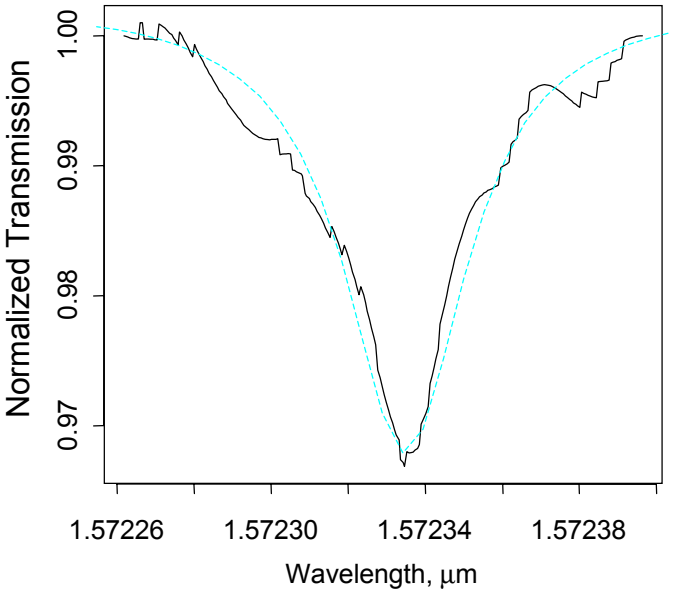

Figure 9. Initial uncalibrated atmospheric CO_2 measurements for the 412m (round trip) horizontal path shown in Figure 8 averaged for 10 seconds. The data were scaled to best match the peak value calculated from the HITRAN database (light blue dashed line). The line center and half-width are in good agreement with the calculated values. A reference cell for calibration will be added to the setup within the next 6 months.

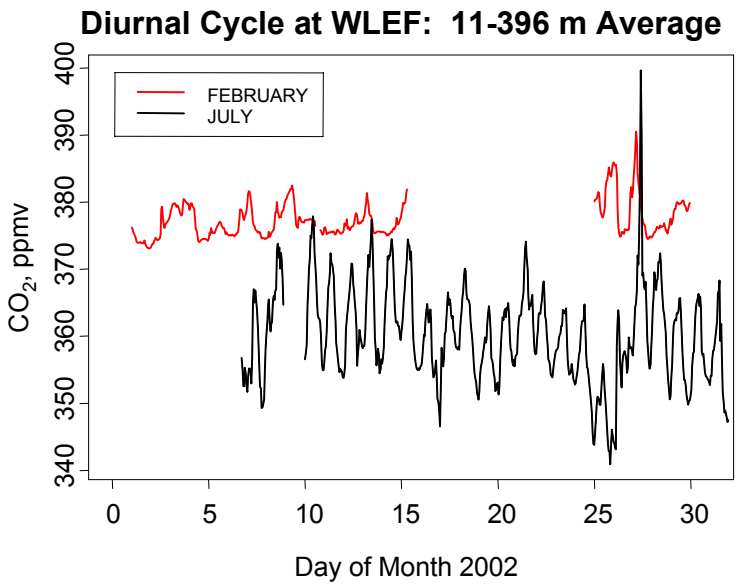

Figure 10. Pressure weighted average CO_2 mixing ratio for the vertical column from 11-396 m at the NOAA CMDL WLEF tall tower monitoring station.

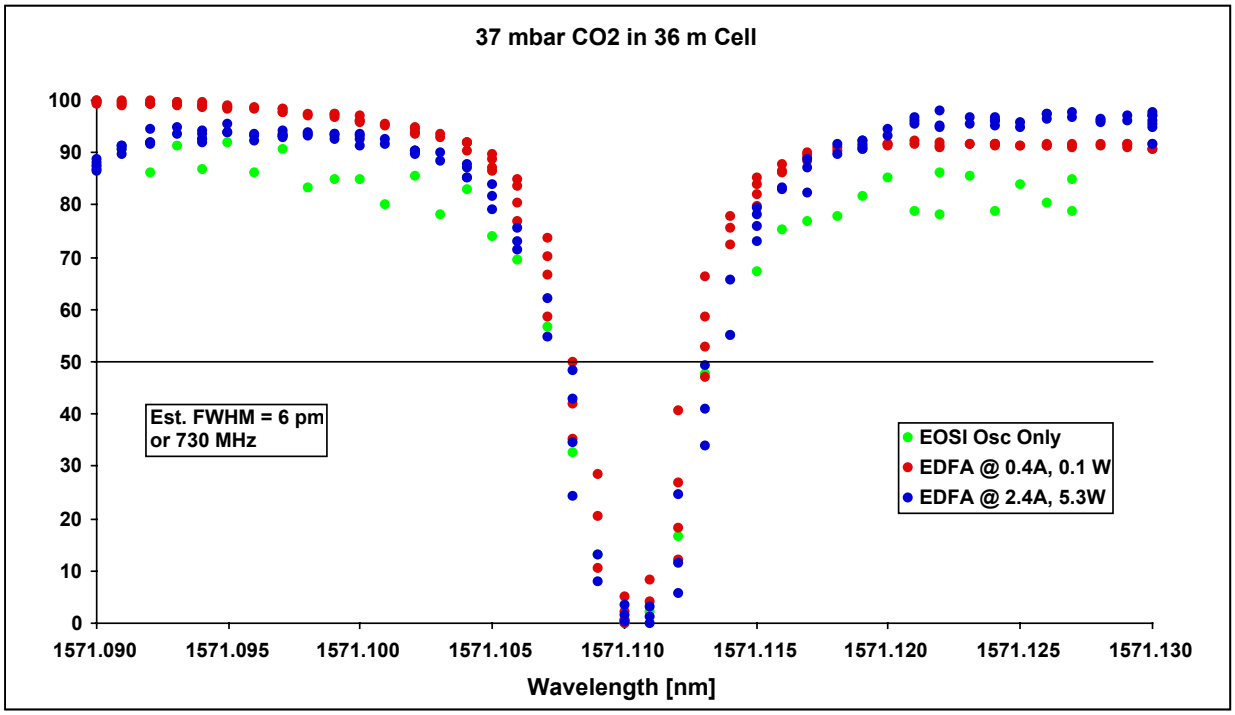

Figure 11. Scan of CO_2 absorption line at 1571.11 nm performed using the EDFA at different power levels. There is no significant broadening of the line when the power is increased from 0.1 W to >5W.

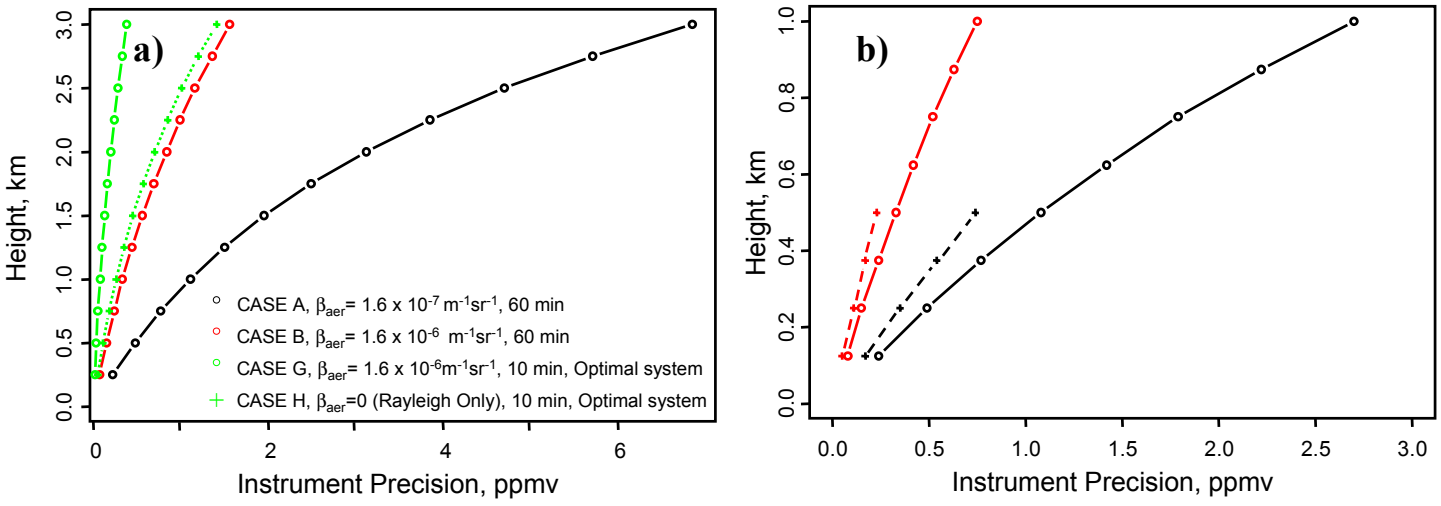

Figure 12. Modeled precision for the proposed system. System parameters for each case are given in Table 2. Nominal cases A-F assume detector quantum efficiency of 2% for the PMT and 10 W of CW output power for the EDFA. Cases G and H represent an "optimal system" showing the impact of using an APD detector with a quantum efficiency of 20% and higher power EDFAs. **(a)** Precision vs. height for cases A, B, G and H up to a maximum altitude of 3 km with vertical resolution of 250 m. **(b)** Daytime (C and D) and nighttime (E and F) cases for the prototype system where the telescope is aligned so that only photons below 1000 m (day) and 500 m (night) enter the field of view of the telescope. The maximum altitudes were chosen to represent nominal PBL heights. Under these conditions, increased vertical resolution of 125 m is possible because the laser can be pulsed at a higher repetition rate. Note that vertical and/or temporal resolution can be sacrificed to achieve higher precision.